



## Effect of Ti content on corrosion behavior of Cu–Ti alloys in 3.5% NaCl solution

Huan WEI<sup>1</sup>, Li-feng HOU<sup>1</sup>, Yan-chao CUI<sup>1</sup>, Ying-hui WEI<sup>1,2</sup>

1. College of Materials Science and Engineering, Taiyuan University of Technology, Taiyuan 030024, China;

2. Shanxi Institute of Technology, Yangquan 045000, China

Received 19 October 2016; accepted 24 April 2017

**Abstract:** The corrosion behavior of the Cu–Ti alloys with different Ti contents in 3.5% (mass fraction) NaCl solution was investigated using electrochemical measurements, immersion tests, mass loss measurements and SEM observation. The results show that Ti dissolved in the Cu matrix changes the corrosion process of the alloys. Pure Cu sample exhibits a typical active–passive–transpassive corrosion behavior. The anodic polarization current densities of the Cu–Ti alloys steadily increase with increasing applied potential, indicating that active dissolution of copper proceeds due to the potential difference in the galvanic coupling of Cu and Ti. The increase of Ti content decreases the corrosion resistance of the Cu–Ti alloys.

**Key words:** Cu–Ti alloy; potentiodynamic polarization; mass loss; immersion test

### 1 Introduction

Copper and its alloys have been extensively used as materials for the preparation of ship apparatus exposed to seawater and marine environments because of their low susceptibility to corrosion [1]. Among the materials used, pure copper is mainly used for conductive parts such as electric circuit boards and wires, Cu–Ni alloys are used for condenser tubing in marine applications, and Cu–Al and Cu–Mn alloys are often used for pump valves, shaft sleeves and pipe fittings. The corrosion behavior of copper and copper alloys has been widely reported [2–7]. Various inhibitors [2–4] and surface films [5] have been used to improve the corrosion resistance of these materials because copper and most copper alloys are poorly passivated in seawater or artificial seawater [6,7]. Even though there are many copper alloys used on ships, there is a need for more variety and the rational application of these materials, which is the ultimate goal in future development.

Dilute Cu–Ti alloys (containing approximately 1%–5% (mass fraction) Ti) are widely known as a substitute for expensive and toxic Cu–Be alloys [8]. They have been used as conductive springs and interconnections with high strength and good electrical

conductivity. Most of the research has focused on their mechanical properties and electrical conductivity [9,10]. Their investigation was focused on the aging process in dilute Cu–Ti alloys, which illustrates the relationship between the hardness, tensile strength, electrical conductivity, and evolution of the microstructure. Because dilute Cu–Ti alloys have attractive mechanical properties and favorable electrical conductivity, it is necessary to gain a better understanding of the underlying corrosion mechanism to be able to expand their application. However, only a few researchers are investigating the corrosion behavior of dilute Cu–Ti alloys [11]. We have explored the correlation of aging precipitates with the corrosion of Cu–4%Ti (mass fraction) alloys in 3.5% (mass fraction) NaCl solution [11]. The effect of Ti dissolved in the Cu matrix on the corrosion behavior of the Cu–Ti alloys is still not clear. A fine scale precipitation  $\text{Cu}_4\text{Ti}$  phase forms in Cu–Ti alloys prepared by solution treatment if the Ti content exceeds 4.0% (mass fraction) [12]. Therefore, Cu–2%Ti and Cu–4%Ti (mass fraction) alloys were used to carry out the study and to eliminate the effect of precipitate on the corrosion behavior of dilute Cu–Ti alloys.

In the present work, we investigated the corrosion behavior of dilute Cu–Ti alloys in 3.5% (mass fraction)

NaCl solution to clarify the mechanism of the corrosion process. The effect of Ti content on the corrosion behavior of the alloys was analyzed using electrochemical techniques and immersion tests.

## 2 Experimental

### 2.1 Preparation of materials

Alloy ingots with a nominal composition of Cu–2%Ti and Cu–4%Ti (mass fraction) (Jiangxi Ke Thai New Materials Co., Ltd., Jiangxi, China) were prepared by melting pure copper (99.99%) and titanium (99.99%) in an argon atmosphere. Cu–2%Ti and Cu–4%Ti alloys were named Cu–2Ti and Cu–4Ti alloys, respectively. To clarify the effect of Ti dissolved in the Cu matrix on the corrosion behavior of the Cu–Ti alloys, pure copper was also tested for comparison. Electrochemical measurements and immersion tests were performed using 10 mm × 10 mm × 6 mm plates that were cut from ingots. The Cu–Ti plates were solution-treated at 1203 K for 2 h and quenched in water at ambient temperature. The pure copper plates were annealed at 973 K for 2 h.

A copper wire was encircled and mounted in epoxy resin. A surface area of 100 mm<sup>2</sup> was exposed for use in the electrochemical tests. Specimens for the electrochemical measurements and immersion tests were ground to 2000 grit, polished, and cleaned with acetone (Chuangdong Chemical Co., Ltd., Chongqing, China) and deionized water before tests. All corrosion measurements were carried out at ambient temperature and conducted in naturally aerated solution. The electrolyte was 3.5% (mass fraction) NaCl solution (3.5 g of NaCl per 96.5 mL deionized water, Chuandong Chemical Co., Ltd., China).

### 2.2 Electrochemical measurements

Electrochemical measurements were conducted using an electrochemical workstation CS350. A conventional three-electrode apparatus was used, which consists of a working electrode, a counter electrode made of platinum foil, and a saturated calomel electrode (SCE) as the reference electrode. Before electrochemical tests, all specimens were immersed in 3.5% NaCl solution for 90 min to stabilize the open circuit potential ( $\varphi_{\text{ocp}}$ ). Following this, impedance measurements were performed at  $\varphi_{\text{ocp}}$  over a frequency range from  $1 \times 10^5$  Hz to  $1 \times 10^{-2}$  Hz with a signal amplitude perturbation of 5 mV. The electrochemical impedance spectroscopy (EIS) data points were fitted using ZSimpWin software. The potential for potentiodynamic polarization test was scanned from –1500 to 1000 mV (vs SCE) at a scan rate of 1 mV/s. All cyclic voltammetry measurements were carried out using a scan rate of 10 mV/s. Each electrochemical experiment was carried out at least three

times, and the results were duplicated.

### 2.3 Immersion tests

After they were ground, polished, cleaned and dried, the specimens were weighed with an electronic balance (QUINTIX213–1CN, Sartorius AG, Germany) to an accuracy of 0.1 mg to find the initial mass ( $m_0$ ). Then, the specimens were immersed in 100 mL of 3.5% NaCl solution for 4 and 8 d at room temperature. The corroded specimens were cleaned with deionized water and dried. The corrosion products were analyzed by TD–3500 X-ray diffraction (XRD). After that, the specimens were immersed in a solution of 0.6 mol/L hydrochloric acid (Chuangdong Chemical Co., Ltd., China) for 3 min to remove the corrosion products, washed quickly with deionized water, dried and then weighed to obtain their final weights ( $m_1$ ). The surface morphologies of the corroded specimens without corrosion products were observed by TESCAN VEGA3 scanning electron microscope (SEM).

## 3 Results

### 3.1 Electrochemical measurements

The impedance measurement results of the Cu, Cu–2Ti and Cu–4Ti alloys are shown in Fig. 1. The Nyquist plots obtained from all of the specimens exhibit a depressed semicircle in the high frequency region followed by a straight line in the low frequency region. The low frequency impedance is known as the Warburg's impedance, which means that the corrosion of both Cu and Cu–Ti alloys is originated from mass transport to some extent. Moreover, the radius of the semicircles observed for the Cu–Ti alloys decreases with increasing Ti content (Fig. 1(a)), demonstrating a decrease in the corrosion resistance. The corresponding Bode plots, shown in Figs. 1(b) and (c), further indicate the variation in the corrosion resistance for all specimens. Both the resistance value and the phase angle decrease with increasing Ti content. The impedance measurement results show that the corrosion resistance degrades as a result of the addition of Ti to copper.

To specifically investigate the electrochemical processes in the interface between metal and electrolyte, impedance parameters were obtained using the software ZSimpwin by fitting Nyquist plots. The equivalent circuit model [11] used for fitting is given in Fig. 2, which is suitable for all samples under study, with the chi-squared values of  $1.694 \times 10^{-4}$ ,  $6.771 \times 10^{-4}$  and  $1.654 \times 10^{-4}$ , corresponding to Cu, Cu–2Ti and Cu–4Ti, respectively. In this work,  $R_1$  represents the solution resistance,  $R_2$  is the resistance of the film formed on the specimen surface, and  $R_3$  is the charge transfer resistance.  $Q_1$  and  $Q_2$  represent the constant phase elements (CPEs).

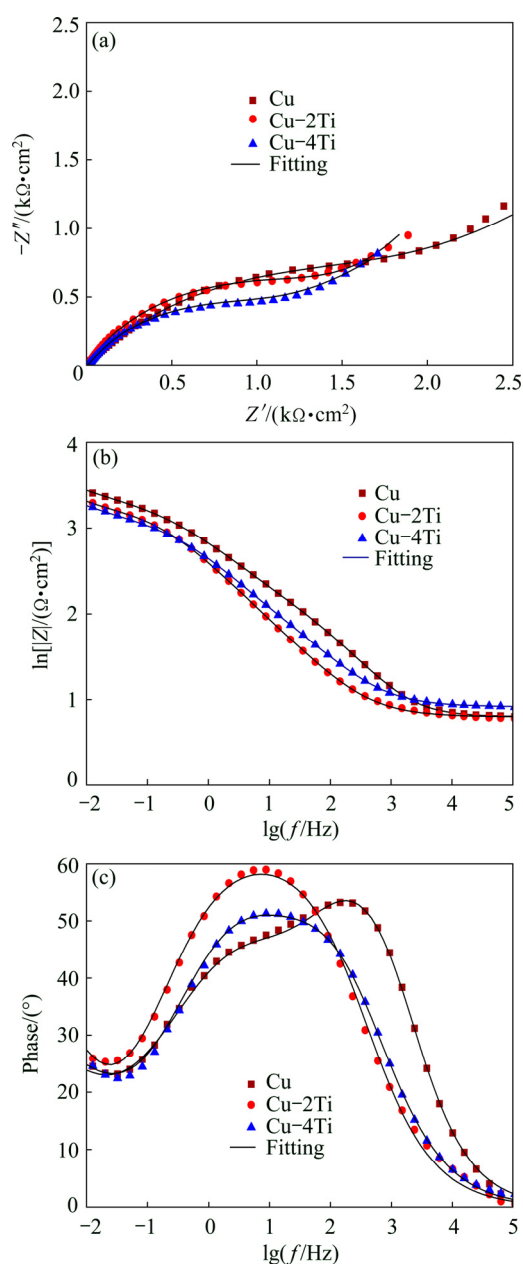


**Fig. 1** Nyquist plots of original and fitted data (a), and Bode plots of original and fitted data (b, c) for Cu, Cu-2Ti and Cu-4Ti alloys in 3.5% NaCl solution

As ideal capacitive behavior is not observed in real interfaces, CPEs are often used as the substitute for capacitors to fit more accurately, representing the impedance behavior of the electric double layer.  $Q_1$  consists of a membrane capacitance  $C_1$  and a deviation

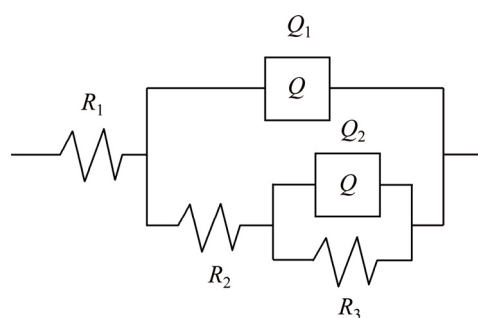


**Fig. 2** Equivalent circuit used to fit electrochemical impedance spectroscopy (EIS) experimental data for Cu, Cu-2Ti and Cu-4Ti alloys in 3.5% NaCl solution

parameter  $n_1$ . The membranes on the pure copper surface in simulated water are generally CuCl and Cu<sub>2</sub>O [13]. Besides, the membranes on the Cu-4Ti surface in 3.5% NaCl solution are also considered to be CuCl and Cu<sub>2</sub>O [11].  $Q_2$  consists of a double-layer capacitance  $C_2$  and a deviation parameter  $n_2$ .  $W$  is Warburg's impedance. The fitted equivalent circuit parameters for all the specimens are listed in Table 1. The value of  $R_3$ , modeling the effective inhibition of the interfacial charge transfer, decreases significantly with increasing Ti content. This accounts for the increased size of the active site available for the copper dissolution reaction. The results show that the increase in Ti content increases the corrosion rate of the alloys in the chloride solution.

Figure 3 shows the potentiodynamic polarization curves for Cu, Cu-2Ti and Cu-4Ti alloys in 3.5% NaCl solution. The corresponding electrochemical parameters of the polarization plots are listed in Table 2. The pure Cu sample shows a typical active-passive-transpassive corrosion behavior, which is associated with the dissolution of copper to ions, the formation of passive Cu<sub>2</sub>O films, and the breakdown of the passive films, respectively. The anodic current of the Cu-2Ti and Cu-4Ti alloys increases steadily with the applied potential, indicating the active dissolution of copper. The corrosion potentials  $\phi_{\text{corr}}$  shifts towards more negative values as the Ti content increases (Table 2), which suggests that the addition of Ti to copper leads to an increase in the active dissolution ability of all the samples. In addition, the variation in the corrosion current density  $J_{\text{corr}}$  also proves that the corrosion resistance of the Cu-Ti alloys is inferior to that of pure

**Table 1** Impedance parameters for Cu, Cu-2Ti and Cu-4Ti alloys in 3.5% NaCl solution at ambient temperature

Alloy	$R_1/(\Omega \cdot \text{cm}^2)$	$R_2/(\Omega \cdot \text{cm}^2)$	$R_3/(\Omega \cdot \text{cm}^2)$	$Q_1$		$Q_2$		$W$
				$C_1/(\mu\text{F} \cdot \text{cm}^{-2})$	$n_1$	$C_2/(\mu\text{F} \cdot \text{cm}^{-2})$	$n_2$	
Cu	6.295	153.8	2051	90.93	0.7945	353.4	0.5914	0.002893
Cu-2Ti	6.266	185.8	1258	621.8	0.7106	0.01114	0.9662	0.004737
Cu-4Ti	8.218	249.5	1006	370.9	0.7072	213.3	0.6873	0.004087

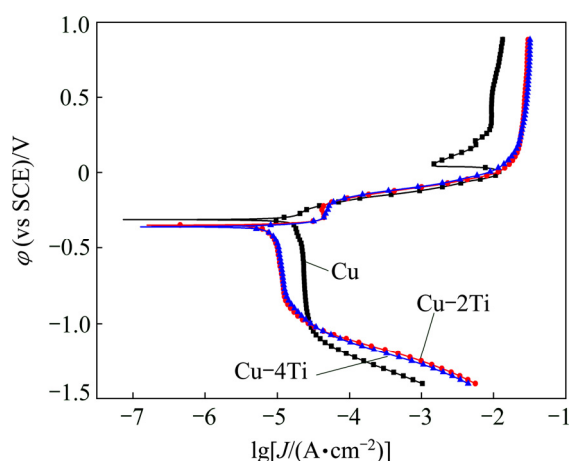


**Fig. 3** Potentiodynamic polarization curves of Cu, Cu-2Ti and Cu-4Ti alloys in 3.5% NaCl solution

**Table 2** Potentiodynamic polarization parameters for Cu, Cu-2Ti and Cu-4Ti alloys in 3.5% NaCl solution

Alloy	$J_{\text{corr}}/(\mu\text{A}\cdot\text{cm}^{-2})$	$\varphi_{\text{corr}}(\text{vs SCE})/\text{mV}$	$\beta_{\text{c}}/(\text{mV}\cdot\text{dec}^{-1})$	$\beta_{\text{a}}/(\text{mV}\cdot\text{dec}^{-1})$
Cu	4.8275	-310.17	-1349.19	86.99
Cu-2Ti	7.6966	-346.66	-592.13	257.33
Cu-4Ti	8.3465	-357.22	-890.78	329.24

copper. In accordance with the impedance measurement results, the polarization results also illustrate that the increase in Ti content decreases the corrosion resistance of the alloys in this work.

### 3.2 Mass loss measurements

The XRD pattern of the corrosion products of Cu-4Ti alloy in 3.5% NaCl solution for 8 d is shown in Fig. 4. The corrosion products are mainly composed of  $\text{Cu}_2\text{O}$  and  $\text{CuCl}$ , which is in accordance with previous study [11].

The mass loss is calculated as follows:

$$C = (m_0 - m_1) / S \quad (1)$$

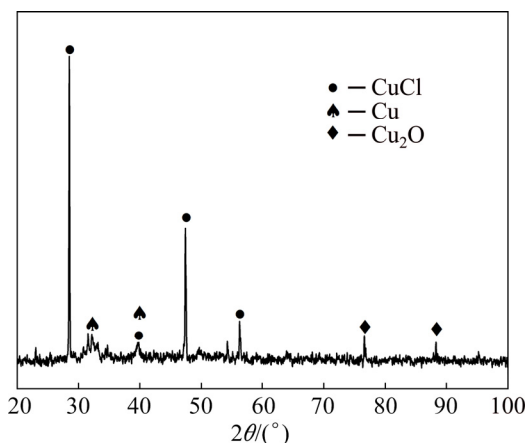


**Fig. 4** XRD pattern of corrosion products of Cu-4Ti alloy in 3.5% NaCl

where  $C$  is the mass loss of the alloy due to corrosion ( $\text{g}/\text{m}^2$ ),  $m_0$  is the original mass (g),  $m_1$  is the final mass without the corrosion products (g), and  $S$  is the surface area ( $\text{m}^2$ ).

Figure 5 shows the mass loss data for Cu, Cu-2Ti and Cu-4Ti alloys during immersion in 3.5% NaCl solution for 8 d. The mass loss increases with prolonged corrosion time for the same alloy. Furthermore, the mass loss gradually increases with increasing Ti content, which agrees with the electrochemical measurements.

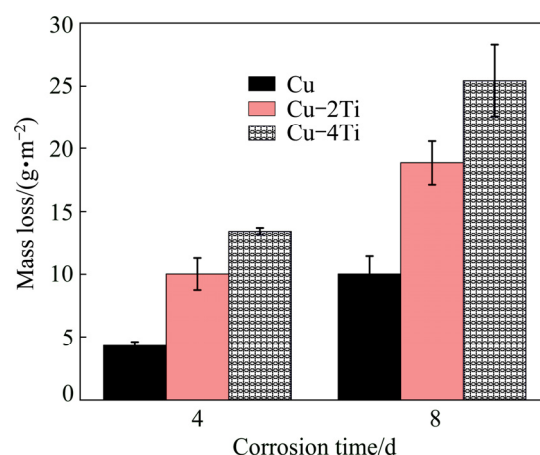


**Fig. 5** Mass losses of Cu, Cu-2Ti and Cu-4Ti alloys during immersion for 8 d

### 3.3 Surface morphology

The surface appearance of the specimens after removing the corrosion products was carefully observed to further investigate the corrosion process. Figure 6 shows SEM morphologies of the alloys after corrosion for 4 and 8 days. After immersion in 3.5% NaCl solution for 4 days, pure Cu is susceptible to intergranular corrosion (Fig. 6(a)). However, both the Cu-2Ti and Cu-4Ti alloys are susceptible to intergranular and pitting corrosion (Figs. 6(c) and (e)). Copper is susceptible to intergranular corrosion in chlorine-containing solutions [14]. The pitting corrosion may be due to the microgalvanic coupling between the copper and titanium atoms in solution treated Cu-Ti alloys. DU et al [15] reported that the potential difference in the galvanic coupling of Cu and Ti could initially partly hinder the surface thermodynamic refining actions, accelerate the diffusion of the aggressive  $\text{Cl}^-$  to the active corrosion sites on copper, and consequently, speed up the initiation of pitting corrosion. As the immersion time is increased to 8 d, copper is close to the general corrosion (Fig. 6(b)). All of the surfaces become rough and porous [2]. Nevertheless, grain boundary grooves are clearly visible, and more and deeper pits are present on the surface of the Cu-2Ti and Cu-4Ti alloys compared with the samples treated for 4 d, as shown in Figs. 6(d) and (f).

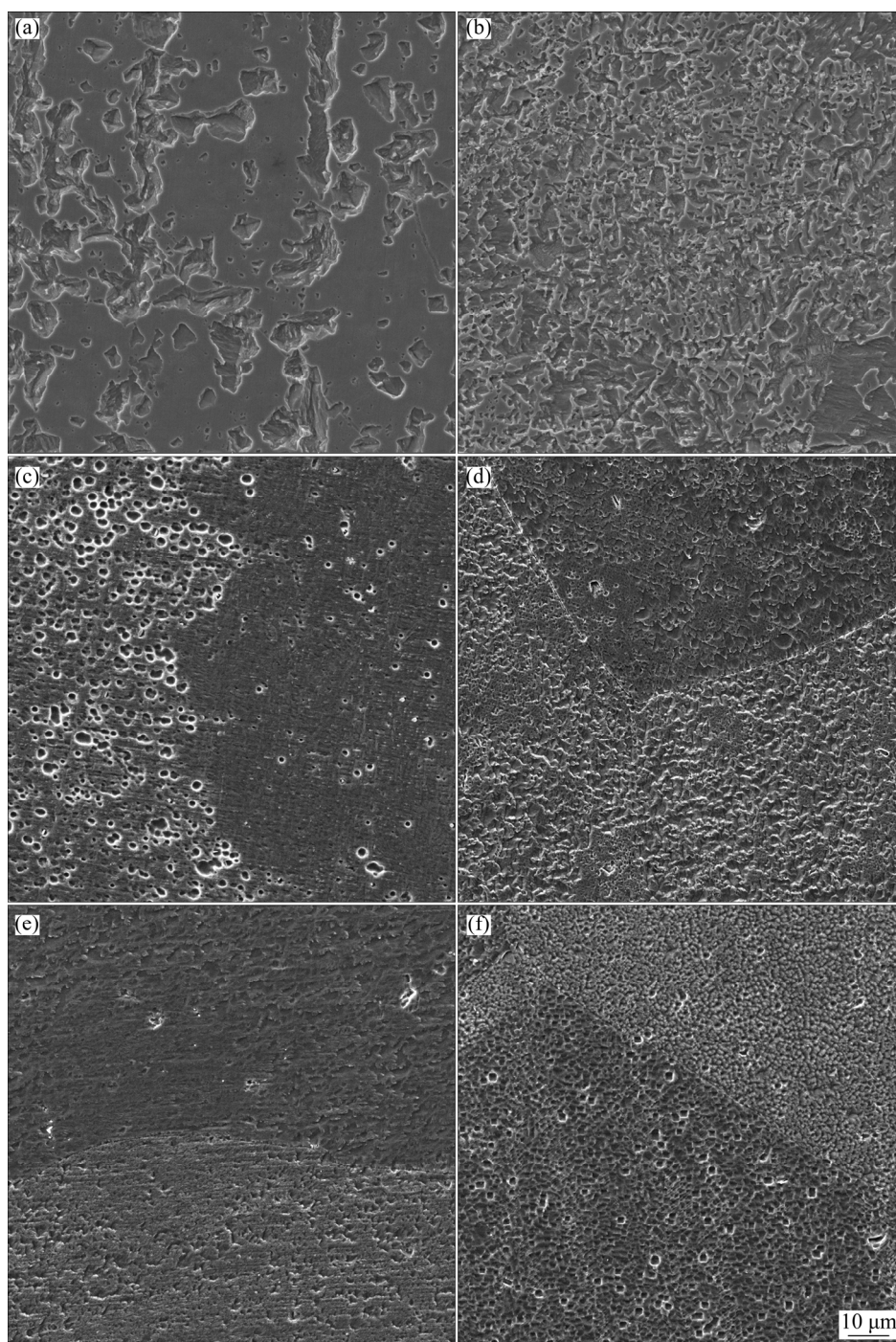


**Fig. 6** SEM images of specimen surfaces corroded for 4 (a, c, e) and 8 d (b, d, f) after removal of corrosion products: (a, b) Cu; (c, d) Cu-2Ti; (e, f) Cu-4Ti

Moreover, the density and size of the pits in the Cu-4Ti alloys were larger than those in the Cu-2Ti alloys. Some grains are selectively attacked whereas others remain intact. This selective corrosion of grains is attributed to the difference in the crystallographic orientation of the surfaces [16]. The surface images of all the samples are consistent with the electrochemical measurements, i.e., the corrosion resistances of all the specimens decrease with increasing Ti content.

## 4 Discussion

As oxidation–reduction reactions occur during cyclic voltammograms measurements, cyclic voltammetry is a common method for determining the microcosmic reaction process on the electrode surface. Thus, the cyclic voltammograms of pure Cu, Cu-2Ti and Cu-4Ti were recorded at a scan rate of 10 mV/s in 3.5%



NaCl solution. The typical cyclic voltammograms for Cu, Cu-2Ti, and Cu-4Ti in 3.5% NaCl solution are shown in Fig. 7. The shapes of the cyclic voltammograms of the Cu and Cu-Ti alloys are considerably different. Each reaction stage is described one by one, and the differences between Cu and the Cu-Ti alloys are discussed below.

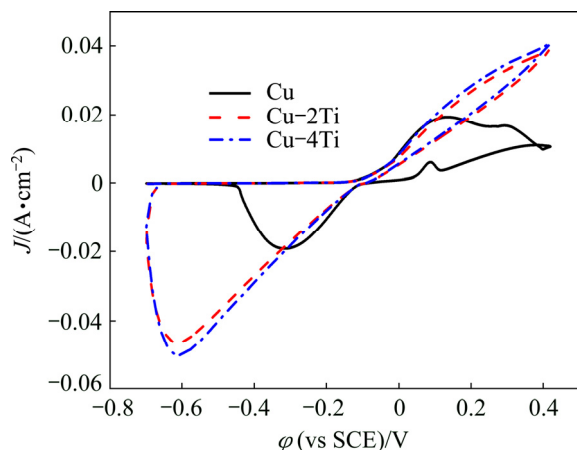
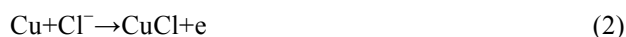


**Fig. 7** Cyclic voltammograms curves of Cu, Cu-2Ti and Cu-4Ti alloys in 3.5% NaCl solution

A transition region is observed before the active dissolution of metal. This transition region, in which the current density is stabilized with increasing potential, is most probably owing to the formation of intermediate species such as  $\text{CuCl}^-$  on the electrode surface [17] according to the following reaction:



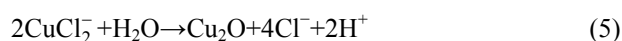
$\text{CuCl}$  is an insoluble product that precipitates on the surface of the electrode and forms a porous  $\text{CuCl}$  film [18]. This stage is observed for all the specimens in this work.

In the anodic region, the current density rapidly increases with increasing potential owing to the formation of soluble  $\text{CuCl}_2^-$  from the dissolution of the adsorbed  $\text{CuCl}$  layer or copper itself, according to the following reactions [19]:



The anodic region is also observed for all the specimens in this work. However, the value of the dissolution current density in the Cu-Ti alloys is larger than that in pure Cu. Furthermore, the current density increases with increasing Ti content.

This suggests that at high concentrations ( $[\text{Cl}^-] > 0.3 \text{ mol/L}$ ), the soluble  $\text{CuCl}_2^-$  hydrolyzes to form a passive  $\text{Cu}_2\text{O}$  layer [19]. The hydrolysis reaction is shown as



The calculated chloride concentration in 3.5% NaCl is 0.6 mol/L. The formation of the  $\text{Cu}_2\text{O}$  layer implies that there is a decrease in the anodic current density, which is observed as a clear peak in the cyclic voltammograms of pure Cu. This phenomenon illustrates that the passivation is present in the pure Cu sample, which is in agreement with the active-passive-transpassive corrosion behavior of pure Cu observed in the potentiodynamic polarization curves (Fig. 3). However, at the same applied potential, the current densities of the Cu-Ti alloys continue to rise, which indicates that the passivation does not occur in the Cu-Ti alloys and the dissolution of copper proceeds. The current density of the Cu-4Ti alloy is higher than that of the Cu-2Ti alloy. In the reverse scan, a clear cathodic peak owing to the reduction of copper ions is observed for all the samples. The cathodic current density increases with increasing Ti content. In addition, the potentiodynamic polarization results show that the anodic current of the Cu-2Ti and Cu-4Ti alloys increases steadily with increasing applied potential, which indicates active dissolution of copper. The cyclic voltammograms are consistent with the potentiodynamic polarization results (Fig. 3). The corrosion resistance of pure Cu is superior to that of the Cu-Ti alloys.

Furthermore, the radius of the semicircles in the plots substantially decreases with increasing Ti content, which demonstrates that the cyclic voltammograms agree well with the impedance measurements (Fig. 1). As the current density increases with increase in Ti content, the number of the active site also increases. Thus, the density of pits increases with increasing Ti content, as shown in Fig. 6. Based on the above reactions, the corrosion products of Cu in 3.5% NaCl solution are  $\text{CuCl}$  and  $\text{Cu}_2\text{O}$ , which is in agreement with Ref. [13]. The corrosion product of the Cu-Ti alloys is predominantly  $\text{CuCl}$  depending on the cyclic voltammograms. However, the corrosion products of the Cu-4Ti alloys in 3.5% NaCl solution after 16 days are  $\text{CuCl}$  and  $\text{Cu}_2\text{O}$  [11]. This may be attributed to a prolonged immersion time, suggesting that the formation of  $\text{Cu}_2\text{O}$  in Cu-Ti alloys is very difficult. All of the electrochemical measurements, immersion tests and surface morphology images are in agreement with the cyclic voltammograms analysis. The increase in Ti content decreases the corrosion resistance of the alloys.

## 5 Conclusions

1) The pure Cu sample shows a typical corrosion behavior including three steps, active-passive-transpassive, which is associated with the dissolution of copper into ions, the formation of passive films  $\text{Cu}_2\text{O}$ , and the breakdown of passive films, respectively.

2) The anodic polarization current densities of the Cu–Ti alloys steadily increase with increasing applied potential, indicating that active dissolution of copper proceeds. The formation of the passive films of  $\text{Cu}_2\text{O}$  in Cu–Ti alloys is difficult, which leads to a decrease in the corrosion resistance as the Ti content increases.

## References

- [1] SYRETT B C. Erosion-corrosion of copper–nickel alloys in sea water and other aqueous environments—A literature review [J]. Corrosion, 1976, 32: 242–252.
- [2] WANG Dan, XIANG Bin, LIANG Yuan-peng, SONG Shan, LIU Chao. Corrosion control of copper in 3.5 wt.% NaCl solution by domperidone: Experimental and theoretical study [J]. Corrosion Science, 2014, 85: 77–86.
- [3] NUNEZ L, REGUERA E, CORVO F, GONZALEZ E, VAZQUEZ C. Corrosion of copper in seawater and its aerosols in a tropical island [J]. Corrosion Science, 2005, 47: 461–484.
- [4] TIAN H, LI W, HOU B. Novel application of a hormone biosynthetic inhibitor for the corrosion resistance enhancement of copper in synthetic seawater [J]. Corrosion Science, 2011, 53: 3435–3445.
- [5] MRTIKOS-HUKOVIC M, BABIC R, SKUGOR I, GRUBAC Z. Copper-nickel alloys modified with thin surface films: Corrosion behaviour in the presence of chloride ions [J]. Corrosion Science, 2011, 53: 347–352.
- [6] MELCHERS R E. Bi-modal trends in the long-term corrosion of copper and high copper alloys [J]. Corrosion Science, 2015, 95: 51–61.
- [7] ZHANG Peng, ZHU Qiang, SU Qian, GUO Bin, CHENG Shu-kang. Corrosion behavior of T2 copper in 3.5% sodium chloride solution treated by rotating electromagnetic field [J]. Transactions of Nonferrous Metals Society of China, 2016, 26: 1439–1446.
- [8] SOFFA W A, LAUGHLIN D E. High-strength age hardening copper–titanium alloys: Redivivus [J]. Progress in Materials Science, 2004, 49: 347–366.
- [9] SEMBOSHI S, NISHIDA T, NUMAKURA H. Microstructure and mechanical properties of Cu–3at.% Ti alloy aged in a hydrogen atmosphere [J]. Materials Science and Engineering A, 2009, 517: 105–113.
- [10] NAGARJUNA S, SRINIVAS M. Grain refinement during high temperature tensile testing of prior cold worked and peak aged Cu–Ti alloys: Evidence of superplasticity [J]. Materials Science and Engineering A, 2008, 498: 468–474.
- [11] WEI Huan, WEI Ying-hui, HOU Li-feng, DANG Ning. Correlation of ageing precipitates with the corrosion behaviour of Cu–4wt.% Ti alloys in 3.5 wt.% NaCl solution [J]. Corrosion Science, 2016, 111: 382–390.
- [12] NAGARJUNA S, SRINIVAS M, BALASUBRAMANIAN K, SARMA D S. The alloy content and grain size dependence of flow stress in Cu–Ti alloys [J]. Acta Materialia, 1996, 44: 2285–2293.
- [13] TASANSUG G, TUKEN T, GIRAY E S, FINDIKKIRAN G, SIGIRCIK G, DEMIRKOL O, ERBIL M. A new corrosion inhibitor for copper protection [J]. Corrosion Science, 2014, 84: 21–29.
- [14] MARTINEZ-LOMBARDIA E, LAPERIRE L, MAURICE V, de GRAEVE I, VERBEKEN K, KLEIN L H, KESTENS L A I, MARCUS P, TERRYH H. In situ scanning tunneling microscopy study of the intergranular corrosion of copper [J]. Electrochemistry Communications, 2014, 41: 1–4.
- [15] DU Xiao-qing, YANG Qing-song, CHEN Yu, YANG Yang, ZHANG Zhao. Galvanic corrosion behavior of copper/titanium galvanic couple in artificial seawater [J]. Transactions of Nonferrous Metals Society of China, 2014, 24: 570–581.
- [16] MIYAMOTO H, HARADA K, MIMAKI T, VINOGRADOV A, HASHIMOTO S. Corrosion of ultra-fine grained copper fabricated by equal-channel angular pressing [J]. Corrosion Science, 2008, 50: 1215–1220.
- [17] DIARD J P, CANUT J M L, GORREC B L, MONTELLA C. Copper electro-dissolution in 1 M HCl at low current densities. I. General steady-state study [J]. Electrochimica acta, 1998, 43: 2469–2483.
- [18] CRUNDWELL F K. A model for the ac-impedance of an electrode coated by a precipitated salt film [J]. Electrochimica Acta, 1991, 36: 1183–1189.
- [19] KEAR G, BARKER B D, STOKES K, WALSH F C. Electrochemical corrosion behaviour of 90–10Cu–Ni alloy in chloride-based electrolytes [J]. Journal of Applied Electrochemistry, 2004, 34: 659–669.

## 钛含量对铜钛合金在 3.5%NaCl 溶液中腐蚀行为的影响

卫 欢<sup>1</sup>, 侯利锋<sup>1</sup>, 崔言超<sup>1</sup>, 卫英慧<sup>1,2</sup>

1. 太原理工大学 材料科学与工程学院, 太原 030024;

2. 山西工程技术学院, 阳泉 045000

**摘 要:** 采用电化学测试、浸泡实验、失重测试和扫描电镜观察研究不同钛含量的铜钛合金在 3.5%(质量分数)NaCl 溶液中的腐蚀行为。结果表明, 溶解在铜基体中的钛改变了铜钛合金的腐蚀过程。纯铜试样呈现典型的活性–钝化–过钝化腐蚀行为。铜钛合金的阳极电流密度随着电势增加而不断增大, 表明铜的活性溶解持续进行, 这主要是由铜与钛之间的电势差造成的。钛含量的增加降低了铜钛合金的耐蚀性。

**关键词:** 铜钛合金; 动电位极化; 质量损失; 浸泡实验

(Edited by Bing YANG)